Microchim Acta (2015) 182:1361–1369
DOI 10.1007/s00604-015-1455-2

ORIGINAL PAPER

Dopamine sensor based on a hybrid material composed of cuprous oxide hollow microspheres and carbon black

Li-Na Wu · Yi-Liang Tan · Li Wang · Sheng-Nan Sun · Zhi-Yu Qu · Jun-Ming Zhang · You-Jun Fan

Received: 29 October 2014 / Accepted: 28 January 2015 / Published online: 18 February 2015

Abstract We report on a novel electrochemical dopamine (DA) sensor based on a glassy carbon electrode (GCE) modified with a hybrid material composed of Cu(I) oxide hollow microspheres and carbon black. The hybrid material was synthesized in a mixed solvent composed of water and the deep eutectic solvent choline chloride/urea, and by in-situ reduction of Cu(II) by ascorbic acid. The surface morphology and structure of the materials were characterized by scanning electron microscopy, transmission electron microscopy and X-ray diffraction. Cyclic voltammetry and chronoamperometry were used to evaluate the electrocatalytic properties of the modified GCE toward DA oxidation in phosphate buffer solution of pH 5.7. The sensor displays a higher electrocatalytic activity toward DA oxidation compared to other modified electrodes. At a working potential of 0.25 V (vs. SCE), the sensor exhibits a rapid response (<3 s) and a wide linear range from 9.9×10^{-8} to 7.08×10^{-4} mol L^{-1}. The detection limit is as low as 3.96×10^{-8} mol L^{-1} (S/N=3). In addition to its high sensitivity, the sensor displays good reproducibility, long-term stability and fair selectivity.

Keywords Electrochemical dopamine sensor · Cu_2O · Hollow microsphere · Deep eutectic solvents

Introduction

Dopamine (DA) is an important catecholamine neurotransmitter in the mammalian central nervous system and plays a key role in the function of central nervous, renal, hormonal and cardiovascular systems [1–3]. The DA concentration in biological systems is usually in the range of 10^{-8} M to 10^{-6} M [4]. Abnormal levels of DA have been associated with several neurological disorders such as Parkinson's disease, schizophrenia, Alzheimer's disease, Huntington's disease, attention deficit hyperactivity disorder and drug addiction [3, 5, 6]. Therefore, the rapid and sensitive detection of DA in biological system is of great clinical importance. At present, various analytical techniques have been developed for the determination of DA that includes mass spectrometry [7], spectrophotometry [8], high performance liquid chromatography (HPLC) [9, 10], chemiluminescence [11] and electrochemical methods [3, 5, 12–15]. Among them, the electrochemical method is considered as a useful approach owing to its high sensitivity, fast response, easy operation, cost-effectiveness and capability of in situ detection [2, 16]. Moreover, the electrochemical detection of DA can be easily realized since it has good electrochemical activity [5].

Transition metal oxides, such as MnO_2 [16], Fe_3O_4 [17], Co_3O_4 [18] and TiO_2 [19] have been used as electrocatalysts for the detection of DA. At the same time, copper oxides including CuO and Cu_2O have attracted intensive interest as promising candidates for electrochemical sensors due to their low cost, environmental friendship and significant catalytic activities [20–24]. For example, Song et al. [21] reported a non-enzymatic H_2O_2 sensor based on CuO nanoflowers whose linear range was from 4.25×10^{-5} to 4×10^{-2} mol L^{-1}, with a detection limit of 0.167 μmol L^{-1}. Liu et al. [24] constructed an electrochemical sensor with the hybrid nanomaterial of Cu_2O nanocubes wrapped by graphene nanosheets, which exhibited the excellent performance toward the detection of glucose and H_2O_2. In particular, several research groups have also explored Cu_xO nanocomposites modified electrodes for the detection of DA [25–27]. Reddy et al. [25]

L.-N. Wu · Y.-L. Tan · L. Wang · S.-N. Sun · Z.-Y. Qu · J.-M. Zhang · Y.-J. Fan (✉)
Guangxi Key Laboratory of Low Carbon Energy Materials, College of Chemistry and Pharmaceutical Sciences, Guangxi Normal University, Guilin 541004, China
e-mail: youjunfan@mailbox.gxnu.edu.cn

synthesized the flake-shaped CuO nanoparticles with enhanced current response for DA. Zhang et al. [27] reported an electrochemical DA sensor based on the Cu_2O/graphene nanocomposite. It is noted that the detection of DA at these Cu_xO-based modified electrodes is almost limited to the voltammetry method. On the other hand, the size and structural morphology of nanoparticles are known to have a significant effect on enhancing the electrochemical response of sensors, and well-controlled nanostructures are thereby essential for achieving efficient electrocatalysts [28]. From this prospect, the shape-controlled synthesis of Cu_xO nanoparticles has attracted enormous attention, and Cu_xO nanoparticles with different shapes were obtained, such as cubes [20, 24], rods [29], nanowires [30, 31], nanoflowers [21, 32] and polyhedra [33]. It is found that the detection performance of sensing electrodes can be improved by changing the morphology of the Cu_xO nanostructures. However, among the various morphologies of Cu_xO nanoparticles, hollow structures have received considerable attention due to their high specific surface area, low density and potential applications in the area of sensing [34–36]. To the best of our knowledge, the studies on Cu_xO hollow microspheres for the amperometric determination of DA have not yet been reported.

Deep eutectic solvents (DESs) are the promising solvents to be used in the shape-controlled synthesis of functional materials due to their unique physicochemical properties, such as high conductivity, viscosity, surface tensions, polarity, thermal stability and negligible vapor pressure [37, 38]. Herein we report the synthesis of Cu_2O hollow microsphere (HMS)/carbon black (CB) hybrid material (Cu_2O HMS/CB) in the DESs/H_2O mixed solvent and its application in the electrochemical determination of DA. The materials were characterized by XRD, SEM and TEM. The Cu_2O HMS/CB composites were used for the fabrication of the modified glassy carbon electrode (GCE) and thus for the electrochemical investigation of DA in PBS solution (pH=5.7). By taking advantages of high electronic conductivity of carbon black and high electrocatalytic activity of Cu_2O hollow microsphere, the Cu_2O HMS/CB composites exhibit strong and sensitive current responses to DA.

Experimental

Reagents

Vulcan XC-72 carbon black (CB) was supplied from Cabot Corporation (http://shminxing027203.11467.com). Dopamine (DA), uric acid (UA) and 5 wt.% Nafion solution were purchased from Sigma-Aldrich (http://www.sigmaaldrich.com/china-mainland/chemistry-product.html). (−)–Epinephrine (+)–bitartrate salt was purchased from J&K Scientific Ltd (Beijing, China) (http://www.jkchemical.com). Choline chloride, urea, absolute ethanol, polyvinylpyrrolidone (PVP), ascorbic acid (AA), $CuSO_4$, NaOH, H_2O_2 and D–glucose were obtained from Sinopharm Chemical Reagent Co. Ltd (Shanghai, China) (http://www.sinoreagent.com). Phosphate buffer saline (PBS, 0.1 mol L^{-1}, pH 5.7) was used as the supporting electrolyte. All the chemicals are of analytical grade and used as received without further purification. All aqueous solutions were prepared using tridistilled water.

Apparatus and measurements

The size and morphology of Cu_2O samples were analyzed by scanning electron microscopy (SEM, LEO-1530) and transmission electron microscopy (TEM, FEI Tecnai-F30). Energy dispersive X-ray (EDX) spectroscopy characterization was conducted on the same apparatus (SEM, LEO-1530), and the Cu_2O content of the Cu_2O HMS/CB composites could be obtained according to the EDX results. X-ray diffraction (XRD) measurements were carried out on an X-ray diffractometer (Rigaku D/MAX 2500 v/pc, Japan) with a Cu Kα radiation source (λ=1.5406 Å). Electrochemical experiments were performed on a CHI 660D electrochemical workstation with a standard three-electrode system comprising a piece of Pt foil (1 cm^2) as auxiliary electrode, a saturated calomel electrode (SCE) as reference electrode, against which all potentials were quoted, and the prepared modified electrode as working electrode. All experiments were carried out at room temperature around 25 °C.

Synthesis of Cu_2O hollow microsphere/carbon black composite

The choline chloride/urea DESs were synthesized according to the previously reported method [38]. In a typical procedure for the synthesis of Cu_2O HMS/CB composite, a DESs/H_2O mixed solvent was first prepared by ultrasonically mixing the DESs and tridistilled water (1:2 in volume). 16 mg ascorbic acid was completely dissolved into 10 mL DESs/H_2O mixed solvent, and the pH value of system was adjusted by the NaOH/DESs solution to 11 (denoted as solution A). Then, 22.3 mg $CuSO_4$, 0.9 g PVP and 25 mg Vulcan XC-72 were added in 20 mL DESs/H_2O mixed solvent under ultrasonic treatment for 30 min, and the pH value of system was adjusted by the NaOH/DESs solution to 11 (denoted as solution B). Subsequently, the solution B was stirred for 15 min at 40 °C, and then the solution A was added dropwise into the solution B. After reaction for 3 h under constant stirring, the as-obtained suspension was allowed to stand overnight. The resultant Cu_2O HMS/CB products were collected by

centrifugation, washed with tridistilled water and absolute ethanol for several times, and dried in vacuum at 60 °C for 24 h. As a comparison, the Cu_2O HMS was prepared with the similar procedure as described above except for the addition of Vulcan XC-72.

Fabrication of modified electrodes

The modified electrode substrate was a glassy carbon electrode (GCE, 5 mm diameter), which was polished sequentially with 5.0 μm, 1.0 μm, 0.3 μm Al_2O_3 powder and then washed ultrasonically in tridistilled water before each experiment. Then 1 mg of the prepared Cu_2O HMS/CB was dispersed ultrasonically in 400 μL Nafion solution (2 wt.%), and 5 μL of the suspension was pipetted and air-dried on the pretreated GCE at room temperature. The resulting modified electrode was denoted as Cu_2O HMS/CB/GCE. In addition, the Cu_2O HMS/GCE and CB/GCE electrodes were also prepared with the similar procedure.

Results and discussion

Physical characterization

In order to analyze the crystal structure and phase purity of the Cu_2O products, the X-ray diffraction measurements were carried out. As shown in Fig. 1, in the case of Cu_2O HMS (curve a), the diffraction peaks at ca. 29.7°, 36.4°, 42.5°, 61.6° and 73.8° originate from the crystal planes of (110), (111), (200), (220) and (311) of the cubic symmetry Cu_2O, respectively [33, 39]. No impurity is detected in this curve, which demonstrates that the high-purity Cu_2O product is successfully synthesized. The average crystallite size was estimated to be 9.7 nm by the Scherrer's equation based on the peak assigned to the (220) plane [40], suggesting that the Cu_2O microspheres

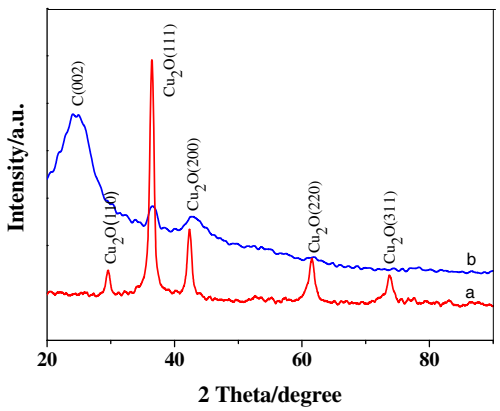

Fig. 1 XRD patterns of Cu_2O HMS (**a**) and Cu_2O HMS/CB (**b**)

are constructed by smaller nanoparticles. For the Cu_2O HMS/CB composite (curve b), the strong peak located at the 2θ value of ca. 24.6° is evidently attributed to the (002) phase of Vulcan XC-72 carbon black [41, 42], and the other three peaks at ca. 36.4°, 42.5° and 63.7° can be ascribed to the diffractions of Cu_2O(111), Cu_2O(200) and Cu_2O(220) planes, respectively. It is noted that, due to the coating of CB, the diffraction signals of Cu_2O become weaker or even disappear.

The morphology of Cu_2O products were further investigated by SEM and TEM methods, and their size distribution was evaluated statistically by measuring the diameter of 200 Cu_2O microspheres in the magnified TEM images. As can be seen from the SEM image of Cu_2O HMS (Fig. 2a), the obtained Cu_2O HMS particles are spherical. The corresponding high magnification SEM image (inset of Fig. 2a) indicates that the Cu_2O microsphere is in fact an agglomerate of abundant Cu_2O nanoparticles. The broken sphere suggests that the spheres are hollow. However, in the SEM image of Cu_2O HMS/CB composite (Fig. 2b), the Cu_2O microspheres are difficult to be observed, which may be due to the embedding of Cu_2O microspheres in CB nanoparticles. Additionally, the TEM image of Cu_2O HMS is shown in Fig. 2c and its particle size distribution is shown in Fig. 2e. The microspheres exhibits paler contrast in the middle region compared to the dark edges, further confirming their hollow structure. The average diameter of the hollow spheres is about 371 nm. The TEM image of Cu_2O HMS/CB composite is shown in Fig. 2d and its particle size distribution is shown in Fig. 2f. It is found that the Cu_2O microspheres are embedded in the CB aggregation, which is in agreement with the XRD results. Their average diameter is about 198 nm, much smaller than that of the Cu_2O HMS product. These results demonstrate that the coating of CB in the Cu_2O HMS/CB composite can not only reduce the size of Cu_2O HMS but also improve the electronic conductivity of the hybrid material effectively. It will be responsible for the enhanced electrocatalytic properties of Cu_2O HMS/CB composite discussed below.

Electrochemical behavior of modified electrodes

The electrochemical behaviors of different modified electrodes were studied by cyclic voltammetry (CV) measurements. Figure 3 shows the CV curves of CB/GCE, Cu_2O HMS/GCE and Cu_2O HMS/CB/GCE electrodes in 0.1 mol L^{-1} PBS (pH=5.7) solution containing 50 μmol L^{-1} DA at a scan rate of 50 mV s^{-1}. As can be seen from the inset of Fig. 3, the Cu_2O HMS/CB/GCE has no redox peaks in blank PBS solution, implying that the Cu_2O HMS/CB/GCE

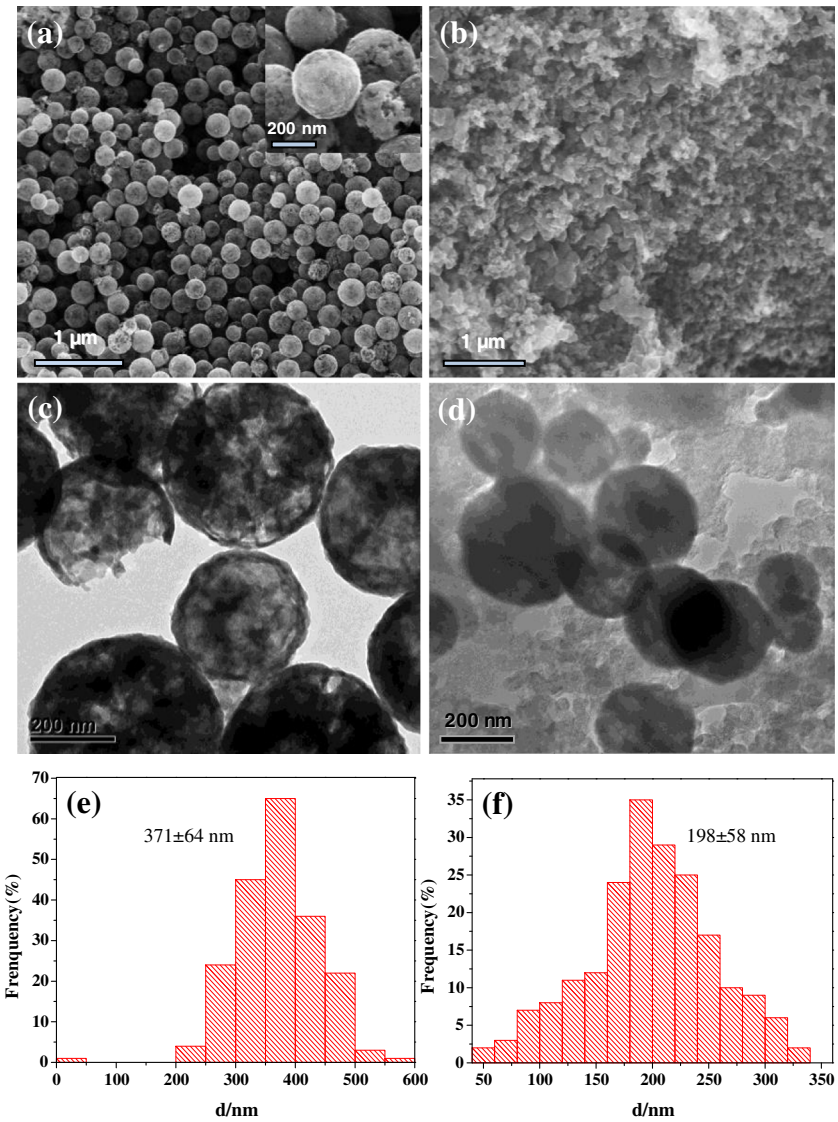

Fig. 2 SEM (**a**), TEM (**c**) images and the size distribution histogram (**e**) of Cu_2O HMS, the inset is the corresponding high-magnification SEM image. SEM (**b**), TEM (**d**) images and the size distribution histogram (**f**) of Cu_2O HMS/CB composite

is non-electroactive in the selected potential region. Upon the addition of 50 μmol L^{-1} DA, it can be observed that the Cu_2O HMS/CB/GCE shows a pair of well-defined peaks with anodic peak potential (E_{pa}) at 0.248 V and cathodic peak potential (E_{pc}) at 0.193 V (Fig. 3a). The corresponding peak potential separation (ΔE_p) is 55 mV, much smaller than that of the Cu_2O HMS/GCE (Fig. 3b, 108 mV) and CB/GCE (Fig. 3c, 78 mV) electrodes, suggesting a fast electron transfer kinetics on the Cu_2O HMS/CB/GCE electrode [27, 43, 44]. Moreover, the anodic and cathodic peak currents of DA on the Cu_2O HMS/CB/GCE are 12.7 and −13.3 μA, respectively, much larger than those on the CB/GCE (3.3 and −3.3 μA) and Cu_2O HMS/GCE (5.8 and −7.6 μA) electrodes. These results indicate that the coating of CB significantly improve the electron transfer rate of Cu_2O HMS and thus enhance the electrocatalytic activity towards DA.

The influence of scan rate on the CV response of Cu_2O HMS/CB/GCE in 0.1 mol L^{-1} PBS solution (pH=5.7) with 50 μmol L^{-1} DA is shown in Fig. 4a. It can be observed that the scan rate affects the positions of the redox peaks and the values of the redox peak currents. With increasing scan rates from 10 to 200 mV s^{-1}, the peak potentials shift to more positive and more negative values for the anodic and cathodic peaks, respectively, and the redox peak currents also increase gradually. The peak potential separation (ΔE_p) become higher with increasing scan rate owing to the increased irreversibility of the electrode process [27, 45]. Furthermore, both the oxidation and reduction peak currents (I_{pa} and I_{pc}) increase linearly with the square root of scan rates (Fig. 4b, linear regression equations: I_{pa} (μA)=3.516 $\nu^{1/2}$–9.995, R^2=0.9929; I_{pc} (μA)=−3.9166 $\nu^{1/2}$+12.5316, R^2=0.9913). These characteristics indicate that the redox behavior of DA at the Cu_2O

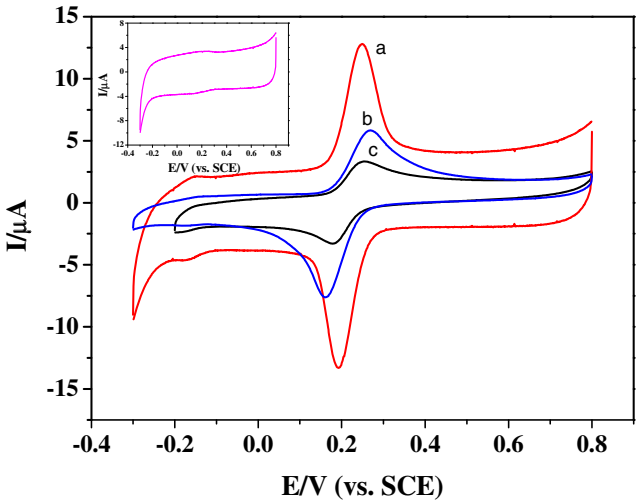

Fig. 3 Cyclic voltammograms of Cu_2O HMS/CB/GCE (**a**), Cu_2O HMS/GCE (**b**) and CB/GCE (**c**) electrodes in 0.1 mol L^{-1} PBS solution (pH=5.7) with 50 μmol L^{-1} DA. Scan rate: 50 mV·s^{-1}. Inset: the cyclic voltammogram of Cu_2O HMS/CB/GCE in 0.1 mol L^{-1} PBS solution (pH=5.7)

HMS/CB/GCE is a typical diffusion-controlled electrochemical process [44, 45].

Effect of solution pH

The effect of pH on the determination of DA in 0.1 mol L^{-1} PBS solution at the Cu_2O HMS/CB/GCE was carefully investigated in the pH range of 4.0–9.5. As shown in Fig. 5a, both anodic and cathodic peak potentials are shifted negatively with the increasing pH values, and the peak current of DA reaches a maximum at about pH=5.7. The results indicate that the electrocatalysis of DA at the composite electrode is a pH dependent reaction and pH 5.7 should be selected as the optimum condition for the electrochemical determination of DA. Figure 5b shows the calibration curve of anodic peak potential versus different pH value. It is found that, in the pH range of 4.0–9.5 the anodic peak potential (E_{pa}) decreases linearly with the increase of pH. The linear regression equation is E_{pa} (V)= 0.6079–0.0639pH with a correlation coefficient of R^2= 0.9951. In addition, the slope value can be calculated to be −63.9 mV/pH using the regression equation, which is close to the theoretical value of −59 mV/pH at 25 °C, indicating a two-proton reaction coupled with a two-electron transfer process [14, 26, 27]. Therefore, the electrochemical reaction of DA at the Cu_2O HMS/CB/GCE electrode can be expressed as the following:

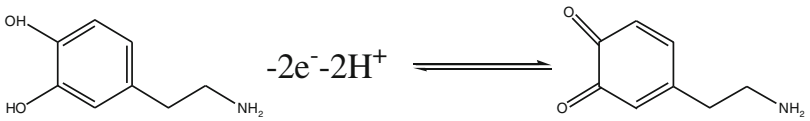

Effect of Cu_2O content in the Cu_2O hollow microsphere/carbon black composite

The Cu_2O content in the Cu_2O HMS/CB composite should play a significant role in the oxidation of DA at the composite modified electrode, so we studied the effect of different Cu_2O mass contents on the current response of Cu_2O HMS/CB/GCE to 50 μmol L^{-1} DA in 0.1 mol L^{-1} PBS solution (pH=5.7) at a scan rate of 50 mV s^{-1}. We synthesized five Cu_2O HMS/CB samples with different Cu_2O mass content by

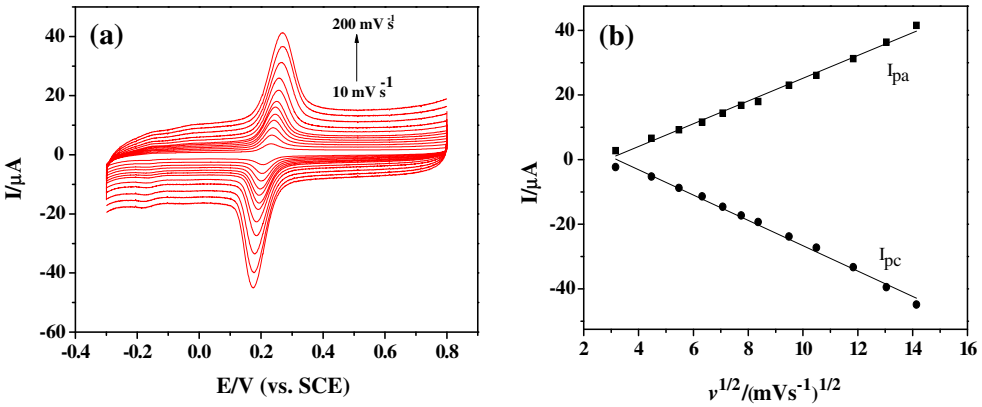

Fig. 4 **a** Cyclic voltammograms of Cu_2O HMS/CB/GCE in 0.1 mol L^{-1} PBS solution (pH=5.7) with 50 μmol L^{-1} DA at different scan rates from 10 mV·s^{-1} to 200 mV·s^{-1}. **b** The plot of the redox peak current versus the square root of scan rate

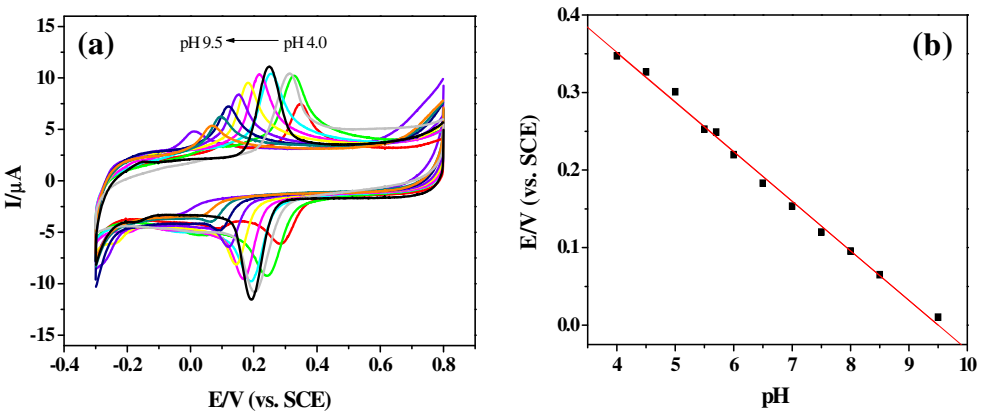

Fig. 5 **a** Cyclic voltammograms of Cu_2O HMS/CB/GCE in 0.1 mol L^{-1} PBS solution with 50 μmol L^{-1} DA at different pH values from 4.0 to 9.5. Scan rate: 50 mV·s^{-1}. **b** The plot of anodic peak potential (E_{pa}) of DA in CV curves versus pH values

changing the amount of $CuSO_4$ precursor, and from the corresponding EDX results their Cu_2O mass contents were determined to be 4.84, 20.46, 27.73, 30.79 and 42.83 %, respectively. As depicted in Fig. 6, the current density was expressed by the normalized current per milligram of Cu_2O loading. It can be seen that, the anodic peak current density increases evidently with the increased Cu_2O mass content, and the maximum response is approached at the Cu_2O content of 20.46 %. Moreover, as described above, smaller peak potential separation (ΔE_p) between the anodic and cathodic peaks responds to faster electron transfer kinetics. When the mass content of Cu_2O in the composite is 20.46 %, the ΔE_p value reaches the minimum, suggesting the fastest electron transfer rate. Thus, 20.46 % Cu_2O was chosen as the optimal mass content for the sensor fabrication.

DA determination of the Cu_2O hollow microsphere/carbon black/GCE sensor

The experiment was performed under the optimized conditions in a stirred system. Figure 7a displays the current-time plot for the Cu_2O HMS/CB/GCE with successive addition of DA into a stirring PBS solution (pH 5.7). As can be seen, the response time is very fast and the steady-state current reaches another steady-state value within 3 s. The present sensor exhibits good linear amperometric response to DA concentration ranging from 9.9×10^{-8} to 7.08×10^{-4} mol L^{-1} (R^2=0.9979), with the sensitivity of 0.0492 μA μM^{-1} and detection limit of 3.96×10^{-8} mol L^{-1} at signal to noise ratio of 3 (Fig. 7b). The performance of the Cu_2O HMS/CB/GCE sensor is compared with those of other published DA electrochemical sensor in Table 1. It can be observed that our proposed sensor exhibits better performance in terms of wide linear range, low detection limit, high sensitivity and fast response time.

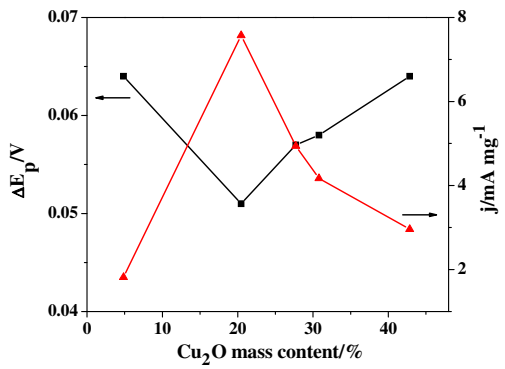

Fig. 6 Effect of Cu_2O mass content in the composite on the ΔE_p value and response current of Cu_2O HMS/CB/GCE electrode in 0.1 mol L^{-1} PBS solution (pH=5.7) with 50 μmol L^{-1} DA. Scan rate: 50 mV·s^{-1}

Reproducibility and stability of the Cu_2O hollow microsphere/carbon black/GCE sensor

The Cu_2O HMS/CB/GCE sensor had a good reproducibility. For eleven electrodes modified identically, the relative standard deviation (RSD) of the current response to 50 μmol L^{-1} DA was 4.67 %. In addition, the storage stability of the sensor was also investigated. When the sensor was stored at the ambient environment and measured intermittently the current response to 50 μmol L^{-1} DA, it still retained 80.3 % of its initial activity after 22 days, indicating that the sensor had a satisfactory stability.

Selectivity of the Cu_2O hollow microsphere/carbon black/GCE sensor

The selectivity of the Cu_2O HMS/CB/GCE sensor was also investigated by using the chronoamperometry technique at the operating potential of 0.25 V. In order to check the effect of substances that might interfere with the sensor performance, five kinds of possible interfering substances, H_2O_2, uric acid, ascorbic acid, glucose and epinephrine were used for measurement in our experiments and the results are shown in Fig. 8. It

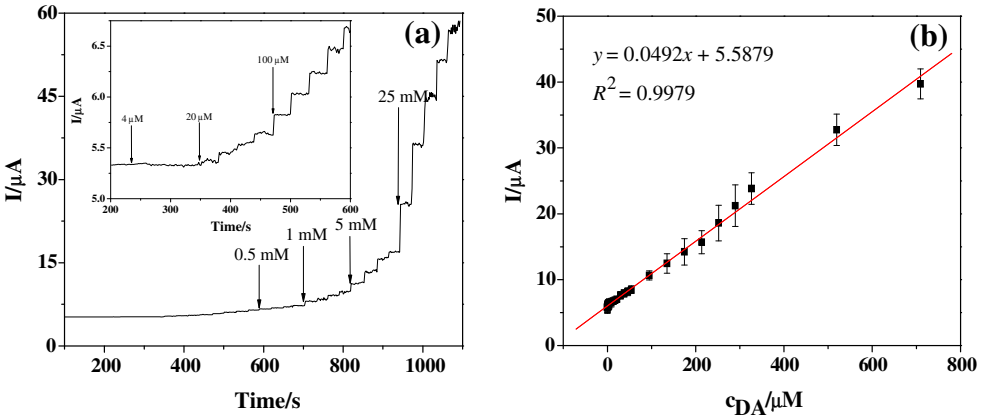

Fig. 7 **a** Amperometric responses of Cu_2O HMS/CB/GCE to the successive addition of DA at the operating potential of 0.25 V in 0.1 mol L^{-1} PBS solution (pH=5.7). **b** The calibration curve of Cu_2O HMS/CB/GCE to different concentration of DA

Table 1 Comparison of present work with other published electrodes for DA determination

Electrode material	Linear range (mol L^{-1})	Detection limit (mol L^{-1})	Response time (s)	Sensitivity (μA $μM^{-1}$)	Reference
TC8A/Au	1×10^{-6}~1×10^{-3}	5×10^{-7}	N/A	0.106	[13]
Fe_3O_4@Au NPs/MCPE	2.0×10^{-6}~9.2×10^{-4}	6.4×10^{-7}	3	N/A	[17]
CuO nanoparticles/MCPE	N/A	5.5×10^{-8}	N/A	N/A	[25]
CuO/MWNTs/Nafion/GCE	1×10^{-6}~8×10^{-5}	4×10^{-7}	N/A	3.0943	[26]
SWNT/NH-GME	9.9×10^{-7}~3.0×10^{-4}	4.2×10^{-7}	N/A	6.04×10^{-5}	[46]
SiO_2/C/CuPc	1.0×10^{-5}~1.4×10^{-4}	6.0×10^{-7}	N/A	1.26×10^{-4}	[47]
MIPs/MWNTs/GCE	6.25×10^{-7}~1.0×10^{-4}	6.0×10^{-8}	N/A	N/A	[48]
$LaPO_4$ nanowires/CPE	2.6×10^{-7}~1.04×10^{-4}	9×10^{-8}	N/A	0.018	[49]
Pt/PEDOT-PB	2×10^{-6}~1×10^{-4}	1.0×10^{-5}	N/A	0.116	[50]
PEDOT/RGO	1×10^{-7}~1.75×10^{-4}	3.9×10^{-8}	N/A	N/A	[51]
Cu_2O HMS/CB/GCE	9.9×10^{-8}~7.08×10^{-4}	3.96×10^{-8}	2.95	0.0492	Present work

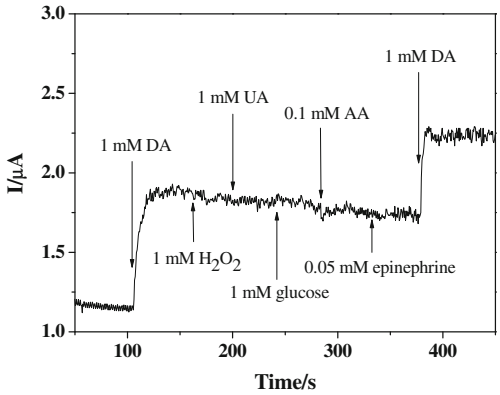

Fig. 8 Chronoamperometry curve of Cu_2O HMS/CB/GCE in 0.1 mol L^{-1} PBS solution (pH=5.7) with successive addition of 1.0 mmol L^{-1} DA, 1.0 mmol L^{-1} H_2O_2, 1.0 mmol L^{-1} UA, 1.0 mmol L^{-1} glucose, 0.1 mmol L^{-1} AA , 0.05 mmol L^{-1} epinephrine and 1.0 mmol L^{-1} DA at applied potential of 0.25 V

can be observed that the five tested interferents could not cause obvious interference to the determination of DA, demonstrating the high selectivity of the Cu_2O HMS/CB/GCE sensor.

Conclusion

The synthesis of Cu_2O HMS/CB hybrid material in the DESs/H_2O mixed solvent and its use in the preparation of amperometric sensor for the detection of DA are reported. SEM, TEM and XRD results reveal that the Cu_2O microspheres are embedded in the CB aggregation and the presence of CB in the Cu_2O HMS/CB composite obviously reduces the size of Cu_2O HMS. The electrocatalytic properties of modified electrodes were studied by using cyclic voltammetry and chronoamperometry methods. Due to high electronic conductivity of CB and high electrocatalytic activity of Cu_2O HMS, the Cu_2O HMS/CB/GCE electrode exhibits higher electrocatalytic activity to DA oxidation compared to other modified electrodes. The Cu_2O HMS/CB/GCE has been employed as

an electrochemical sensor for determination of DA in the wide range from 9.9×10^{-8} to 7.08×10^{-4} mol L^{-1} with a low detection limit of 3.96×10^{-8} mol L^{-1} (S/N=3). In addition, the sensor also displays advantages including high sensitivity, good reproducibility, long-term stability and selectivity. The work reported here provides a new platform for preparing an amperometric DA sensor with high performance and low cost.

Acknowledgments This work was supported by the National Natural Science Foundation of China (21463007, 21263002), Guangxi Natural Science Foundation of China (2013GXNSFAA019024, 2014GXNSFFA118003), the S&T Project of Guangxi Education Department of China (2013YB026), BAGUI Scholar Program (2014A001) and Project of Talents Highland of Guangxi Province.

References

1. van Staden JF, van Staden RIS (2012) Flow-injection analysis systems with different detection devices and other related techniques for the in vitro and in vivo determination of dopamine as neurotransmitter: a review. Talanta 102:34
2. Zhang M, Liao CZ, Yao YL, Liu ZK, Gong FF, Yan F (2014) High-performance dopamine sensors based on whole graphene solution-gated transistors. Adv Funct Mater 24:978
3. Lin L, Du JM, Li SJ, Yuan BQ, Han HX, Jing M, Xia N (2013) Amplified voltammetric detection of dopamine using ferrocene-capped gold nanoparticle/streptavidin conjugates. Biosens Bioelectron 41:730
4. Kim J, Jeon M, Paeng KJ, Paeng IR (2008) Competitive enzyme-linked immunosorbent assay for the determination of catecholamine, dopamine in serum. Anal Chim Acta 619:87
5. Njagi J, Chernov MM, Leiter JC, Andreescu S (2010) Amperometric detection of dopamine in vivo with an enzyme based carbon fiber microbiosensor. Anal Chem 82:989
6. Maina FK, Mathews TA (2010) Functional fast scan cyclic voltammetry assay to characterize dopamine D2 and D3 autoreceptors in the mouse striatum. ACS Chem Neurosci 1:450
7. Kim HR, Kim TH, Hong SH, Kim HG (2012) Direct detection of tetrahydrobiopterin (BH4) and dopamine in rat brain using liquid chromatography coupled electrospray tandem mass spectrometry. Biochem Biophys Res Commun 419:632
8. Nezhad MRH, Tashkhourian J, Khodaveisi J (2010) Sensitive spectrophotometric detection of dopamine, levodopa and adrenaline using surface plasmon resonance band of silver nanoparticles. J Iran Chem Soc 7:83
9. Hows MEP, Lacroix L, Heidbreder C, Organ AJ, Shah AJ (2004) High-performance liquid chromatography/tandem mass spectrometric assay for the simultaneous measurement of dopamine, norepinephrine, 5-hydroxytryptamine and cocaine in biological samples. J Neurosci Methods 138:123
10. Li N, Guo JZ, Liu B, Cui H, Mao LQ, Lin YQ (2009) Determination of monoamine neurotransmitters and their metabolites in a mouse brain microdialysate by coupling high-performance liquid chromatography with gold nanoparticle initiated chemiluminescence. Anal Chim Acta 645:48
11. Cui R, Gu YP, Bao L, Zhao JY, Qi BP, Zhang ZL, Xie ZX, Pang DW (2012) Near-infrared electrogenerated chemiluminescence of ultrasmall Ag_2Se quantum dots for the detection of dopamine. Anal Chem 84:8932
12. Keithley RB, Takmakov P, Bucher ES, Belle AM, Owesson-White CA, Park J, Wightman RM (2011) Higher sensitivity dopamine measurements with faster-scan cyclic voltammetry. Anal Chem 83:3563
13. Zheng G, Chen M, Liu XY, Zhou J, Xie J, Diao GW (2014) Self-assembled thiolated calix[n]arene (n=4, 6, 8) films on gold electrodes and application for electrochemical determination dopamine. Electrochim Acta 136:301
14. Palanisamy S, Ku SH, Chen SM (2013) Dopamine sensor based on a glassy carbon electrode modified with a reduced graphene oxide and palladium nanoparticles composite. Microchim Acta 180:1037
15. Khan A, Khan AAP, Asiri AM, Rub MA, Rahman MM, Ghani SA (2014) In vitro studies of carbon fiber microbiosensor for dopamine neurotransmitter supported by copper-graphene oxide composite. Microchim Acta 181:1049
16. Huang Y, Cheng CM, Tian XQ, Zheng BZ, Li Y, Yuan HY, Xiao D, Choi MMF (2013) Low-potential amperometric detection of dopamine based on MnO_2 nanowires/chitosan modified gold electrode. Electrochim Acta 89:832
17. Qiu JD, Xiong M, Liang RP, Peng HP, Liu F (2009) Synthesis and characterization of ferrocene modified Fe_3O_4@Au magnetic nanoparticles and its application. Biosens Bioelectron 24:2649
18. Elhag S, Ibupoto ZH, Liu X, Nur O, Willander M (2014) Dopamine wide range detection sensor based on modified Co_3O_4 nanowires electrode. Sensors Actuators B Chem 203:543
19. Majidi MR, Asadpour-Zeynali K, Gholizadeh S (2010) Nanobiocomposite modified carbon-ceramic electrode based on nano-TiO_2-plant tissue and its application for electrocatalytic oxidation of dopamine. Electroanalysis 22:1772
20. Zhang L, Li H, Ni Y, Li J, Liao K, Zhao G (2009) Porous cuprous oxide microcubes for non-enzymatic amperometric hydrogen peroxide and glucose sensing. Electrochem Commun 11:812
21. Song MJ, Hwang SW, Whang D (2010) Non-enzymatic electrochemical CuO nanoflowers sensor for hydrogen peroxide detection. Talanta 80:1648
22. Reitz E, Jia W, Gentile M, Wang Y, Lei Y (2008) CuO nanospheres based nonenzymatic glucose sensor. Electroanalysis 20:2482
23. Guo Z, Seol ML, Kim MS, Ahn JH, Choi YK, Liu JH, Huang XJ (2012) Hollow CuO nanospheres uniformly anchored on porous Si nanowires: preparation and their potential use as electrochemical sensors. Nanoscale 4:7525
24. Liu M, Liu R, Chen W (2013) Graphene wrapped Cu_2O nanocubes: non-enzymatic electrochemical sensors for the detection of glucose and hydrogen peroxide with enhanced stability. Biosens Bioelectron 45:206
25. Reddy S, Kumara SBE, Jayadevappa H (2012) CuO nanoparticle sensor for the electrochemical determination of dopamine. Electrochim Acta 61:78
26. Yang S, Li G, Yin Y, Yang R, Li J, Qu L (2013) Nano-sized copper oxide/multi-wall carbon nanotube/Nafion modified electrode for sensitive detection of dopamine. J Electroanal Chem 703:45
27. Zhang F, Li Y, Gu Y, Wang Z, Wang C (2011) One-pot solvothermal synthesis of a Cu_2O/graphene nanocomposite and its application in an electrochemical sensor for dopamine. Microchim Acta 173:103
28. Sanghavi BJ, Wolfbeis OS, Hirsch T, Swami NS (2015) Nanomaterial-based electrochemical sensing of neurological drugs and neurotransmitters. Microchim Acta 182:1
29. Wang X, Hu C, Liu H, Du G, He X, Xi Y (2010) Synthesis of CuO nanostructures and their application for nonenzymatic glucose sensing. Sensors Actuators B Chem 144:220
30. Zhuang Z, Su X, Yuan H, Sun Q, Xiao D, Choi MMF (2008) An improved sensitivity non-enzymatic glucose sensor based on a CuO nanowire modified Cu electrode. Analyst 133:126
31. Jia W, Guo M, Zheng Z, Yu T, Wang Y, Rodriguez EG, Lei Y (2008) Vertically aligned CuO nanowires based electrode for amperometric detection of hydrogen peroxide. Electroanalysis 20:2153

32. Umar A, Rahman MM, Al-Hajry A, Hahn YB (2009) Enzymatic glucose biosensor based on flower-shaped copper oxide nanostructures composed of thin nanosheets. Electrochem Commun 11:278
33. Zhang X, Wang G, Gu A, Wu H, Fang B (2008) Preparation of porous Cu_2O octahedron and its application as L-Tyrosine sensors. Solid State Commun 148:525
34. Wang B, Luo L, Ding Y, Zhao D, Zhang Q (2012) Synthesis of hollow copper oxide by electrospinning and its application as a non-enzymatic hydrogen peroxide sensor. Colloids Surf B 97:51
35. Khan SB, Faisal M, Rahman MM, Abdel-Latif IA, Ismail AA, Akhtar K, Al-Hajry A, Asiri AM, Alamry KA (2013) Highly sensitive and stable phenyl hydrazine chemical sensors based on CuO flower shapes and hollow spheres. New J Chem 37:1098
36. Sui Y, Zhang Y, Fu W, Yang H, Zhao Q, Sun P, Ma D, Yuan M, Li Y, Zou G (2009) Low-temperature template-free synthesis of Cu_2O hollow spheres. J Cryst Growth 311:2285
37. Wei L, Fan YJ, Tian N, Zhou ZY, Zhao XQ, Mao BW, Sun SG (2012) Electrochemically shape-controlled synthesis in deep eutectic solvents — a new route to prepare Pt nanocrystals enclosed by high-index facets with high catalytic activity. J Phys Chem C 116:2040
38. Wei L, Fan YJ, Wang HH, Tian N, Zhou ZY, Sun SG (2012) Electrochemically shape-controlled synthesis in deep eutectic solvents of Pt nanoflowers with enhanced activity for ethanol oxidation. Electrochim Acta 76:468
39. Zhou LS, Shen FP, Tian XK, Wang DH, Zhang T, Chen W (2013) Stable Cu_2O nanocrystals grown on functionalized graphene sheets and room temperature H_2S gas sensing with ultrahigh sensitivity. Nanoscale 5:1564
40. Zhu HT, Wang JX, Xu GY (2009) Fast synthesis of Cu_2O hollow microspheres and their application in DNA biosensor of hepatitis B virus. Cryst Growth Des 9:633
41. Feng L, Yao S, Zhao X, Yan L, Liu C, Xing W (2012) Electrocatalytic properties of Pd/C catalyst for formic acid electrooxidation promoted by europium oxide. J Power Sources 197:38
42. Gattia DM, Antisari MV, Giorgi L, Marazzi R, Piscopiello E, Montone A, Bellitto S, Licoccia S, Traversa E (2009) Study of different nanostructured carbon supports for fuel cell catalysts. J Power Sources 194:243
43. Zhang YQ, Fan YJ, Cheng L, Fan LL, Wang ZY, Zhong JP, Wu LN, Shen XC, Shi ZJ (2013) A novel glucose biosensor based on the immobilization of glucose oxidase on layer-by-layer assembly film of copper phthalocyanine functionalized graphene. Electrochim Acta 104:178
44. Angeles GA, Lopez BP, Pardave MP, Silva MTR, Alegret S, Merkoci A (2008) Enhanced host-guest electrochemical recognition of dopamine using cyclodextrin in the presence of carbon nanotubes. Carbon 46:898
45. Niu XL, Yang W, Guo H, Ren J, Gao JZ (2013) Highly sensitive and selective dopamine biosensor based on 3,4,9,10-perylene tetracarboxylic acid functionalized graphene sheets/multi-wall carbon nanotubes/ionic liquid composite film modified electrode. Biosens Bioelectron 41:225
46. Cao XH, Zhang LX, Cai WP, Li YQ (2010) Amperometric sensing of dopamine using a single-walled carbon nanotube covalently attached to a conical glass micropore electrode. Electrochem Commun 12:540
47. Rahim A, Barros SBA, Kubota LT, Gushikem Y (2011) SiO_2/C/Cu(II) phthalocyanine as a biomimetic catalyst for dopamine monooxygenase in the development of an amperometric sensor. Electrochim Acta 56:10116
48. Kan XW, Zhou H, Li C, Zhu AH, Xing ZL, Zhao Z (2012) Imprinted electrochemical sensor for dopamine recognition and determination based on a carbon nanotube/polypyrrole film. Electrochim Acta 63:69
49. Zhou YZ, Zhang HY, Xie HD, Chen B, Zhang L, Zheng XH, Jia P (2012) A novel sensor based on $LaPO_4$ nanowires modified electrode for sensitive simultaneous determination of dopamine and uric acid. Electrochim Acta 75:360
50. Lupu S, Lete C, Marin M, Totir N, Balaure PC (2009) Electrochemical sensors based on platinum electrodes modified with hybrid inorganic-organic coatings for determination of 4-nitrophenol and dopamine. Electrochim Acta 54:1932
51. Wang W, Xu G, Cui XT, Sheng G, Luo X (2014) Enhanced catalytic and dopamine sensing properties of electrochemically reduced conducting polymer nanocomposite doped with pure graphene oxide. Biosens Bioelectron 58:153